

Cross-Correlation of Nuclear Quadrupolar Interactions as a Probe in Structure Elucidation: Liquid-Phase Nuclear Magnetic Resonance Studies on Bis(hexamethyldisilylamido)mercury(II)

Piotr Bernatowicz,[†] Sławomir Szymański,^{*,†} and Bernd Wrackmeyer[‡]

Institute of Organic Chemistry, Polish Academy of Sciences, Kasprzaka 44/52, PL-01-224 Warsaw, Poland, and Inorganic Chemistry II, Bayreuth University, D-95440 Bayreuth, Germany

Received: February 22, 2001; In Final Form: April 20, 2001

The values of longitudinal nuclear spin relaxation rates for the ¹⁹⁹Hg (spin-1/2) and ¹⁴N (spin-1) nuclei and of the quadrupolar cross-correlation coefficient for the ¹⁴N nuclei are determined for a toluene solution of bis(hexamethyldisilylamido)mercury(II) in a broad temperature range. Estimates of the latter quantity were obtained from iterative line shape fits of the ¹⁹⁹Hg resonance signals. Sensitivity of the ¹⁹⁹Hg resonances to the quadrupolar cross-correlations is because in the temperature range investigated the quadrupolar relaxation rates of the ¹⁴N nuclei become comparable to the ¹⁹⁹Hg-¹⁴N scalar coupling. The data obtained are shown to be consistent with the structure in which the Si₂N-Hg-NSi₂ skeleton maintains *D*_{2d} geometry on the time scale of the overall molecular reorientation. Under a well-justified assumption involving the extent of the possible anisotropy of the latter, the principal axes of the ¹⁴N electric field gradient tensors, corresponding to the gradients of maximum absolute values, can be unambiguously located along the direction of the N–Hg–N chain. The value of the electric field gradient asymmetry parameter, calculated from the experimental data assuming perfectly isotropic reorientation, amounts to 0.62. The present study seems to provide the first evidence of the utility of quadrupolar cross-correlation effects for structural studies in isotropic liquids.

Introduction

The bulk of literature data documenting usefulness of nuclear spin relaxation phenomena for structural studies in solutions involves the dipolar relaxation mechanism. This is due to an explicit dependence of the dipolar relaxation rates on the internuclear distances. Relaxation mechanisms arising from fluctuating interactions that engage single nuclei, such as nuclear quadrupole–electric field gradient (EFG) and nuclear dipole–external magnetic field modulated by chemical shift anisotropy (CSA), may seem to be of limited interest in this context because of a lack of any straightforward dependence on the intramolecular distances. However, randomly modulated interactions of any sort that lead to relaxation can interfere with one another to produce the so-called cross-correlation contributions to relaxation. Cross-correlations may even arise between interactions that operate in remote parts of the molecule. Thus, although they still do not bear any functional dependence on the distances, in some cases they may provide crucial structural information. According to a recent review on the cross-correlation effects,¹ in the past the research was predominantly concentrated on the instances where the cross-correlated interactions share one nucleus in common; cross-correlation of fluctuating dipolar coupling between a ¹³C nucleus and an adjacent proton, and fluctuating, CSA-mediated interaction of the former is a typical example. Little attention was devoted to cross-correlation effects in systems of quadrupolar nuclei interacting with the EFGs. The methods of evaluation of such

effects that were once developed by Vold et al.^{2,3} involve partially ordered systems the NMR spectra of which exhibit resolved quadrupolar splittings. The specific case of symmetric diatomics with large rotational constants, dissolved in liquid crystalline media, where the signal splittings can be different for the ortho and para species, was addressed by ter Beek and Burnell.⁴ For isotropic fluids, where the quadrupolar splittings do not occur, an appropriate general methodology has not been worked out yet. However, in systems where resonance signals of the quadrupolar nuclei overlap, at least partially, there exists a possibility to evaluate the interesting effects by examining the line shape of a “spy” nucleus, preferably a spin-1/2 nucleus, that is scalar coupled to these quadrupolar nuclei, provided that the quadrupolar longitudinal relaxation rates are not prohibitively large in comparison with the coupling constants. This is an inference from extensive line shape simulations performed by us, based on the Bloch–Wangsness–Redfield (BWR) theory of nuclear spin relaxation in multispin systems.^{5,6} For systems where the quadrupolar nuclei are magnetically equivalent certain aspects of the above line shape problem that are crucial for obtaining an unbiased estimate of the cross-correlation coefficient, *r*, were thoroughly discussed in our former works.^{7–9} Actually, our results for a benzosenadiazole derivative dissolved in aromatic solvents, obtained from line shape fittings of ⁷⁷Se spectra,⁸ seem to be the only unbiased estimates of quadrupolar cross-correlations in isotropic fluids reported so far.

In the present work, the approach of ref 8, augmented with standard NMR relaxation measurements, will be applied to the problem of solution structure of bis(hexamethyldisilylamido)mercury(II) **1**. In neat liquids, the structure of **1** and its cadmium, **2**, and zinc, **3**, analogues were once investigated using IR/Raman spectroscopy.¹⁰ For all these compounds, it was concluded that

* To whom correspondence should be addressed. E-mail: sszym@icho.edu.pl.

[†] Polish Academy of Sciences.

[‡] Bayreuth University. E-mail: b.wrack@uni-bayreuth.de; fax: +49 921 55 2157.

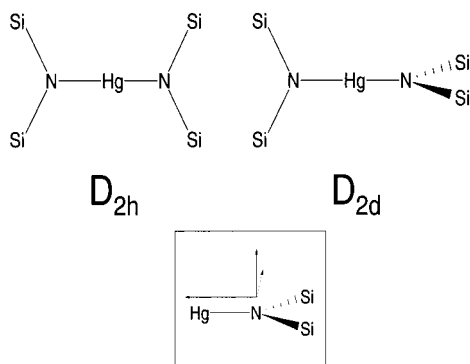


Figure 1. D_{2h} and D_{2d} conformations of **1**. Inset: Principal axes of the EFG tensors of the ^{14}N nuclei.

the N–M–N chains are linear, and the MNSi_2 fragments are planar. Regarding the mutual orientation of the MNSi_2 ligands, the IR/Raman mutual exclusion principle did not allow to discriminate between the eclipsed (D_{2h} symmetry) and staggered (D_{2d} symmetry) conformations (see Figure 1).¹⁰ In gas phase, of the models with assumed D_{2h} and D_{2d} geometries of the $\text{Si}_2\text{NMNSi}_2$ skeleton only the latter could be satisfactorily brought into agreement with the experimental electron diffraction (ED) data for **1**,¹¹ **2**,¹² and **3**.¹³ However, in the final structure refinements, it had proven advantageous to postulate the occurrence of large amplitude librations around the N–M–N axis. The estimated librational energy barriers were low, about $8 \pm 4 \text{ kJ mol}^{-1}$, and their origin was attributed to intramolecular steric rather than electronic effects.¹⁴ In view of these findings, a straightforward extension of the above conclusions to the solution structures of the compounds in question did not seem justified. This was one of our motivations to undertake the present study on the solution structure of **1**.

Experimental Section

The compound **1**, which is a nonvolatile liquid under ambient conditions (mp 12°C), was synthesized and purified according to a published procedure.¹⁰ All of the NMR data referred to in the present work were obtained for a 1 mol/L solution of **1** in toluene- d_8 , sealed in NMR tube (o.d. 5 mm) under argon at ambient pressure. NMR measurements were performed on a Bruker DRX 250 and Bruker DRX 500 MHz spectrometers. All variable temperature measurements were performed on the latter machine equipped with temperature control unit BVT 3000. The sample temperature was determined from reads of a thermocouple placed within the NMR probehead which were calibrated against the methanol (for $T < 303 \text{ K}$) and ethylene glycol ($T > 303 \text{ K}$) chemical shift thermometers. The ^{199}Hg and ^{14}N spectra to be subject to iterative line shape analysis were obtained by collecting data from 100 000–400 000 and 4000–10000 scans, respectively. The spectra of ^{15}N at natural abundance, measured to determine scalar couplings (J-couplings) to the nitrogen atoms, were obtained by collecting 10 000 scans. The magnitude of the ^{14}N – ^{15}N coupling constant was estimated from line shape broadening of the ^{15}N signal and from longitudinal relaxation time of the ^{14}N nucleus.¹⁵ Values of the scalar coupling constants that are relevant for the line shape analysis are listed in Table 1.

Evaluation of Quadrupolar Cross-Correlations. In the molecule of **1**, the ^{199}Hg nucleus is the only candidate for the “spy” nucleus whose resonance line shape is to provide information on the quadrupolar cross-correlation coefficient, r , for the pair of isochronous ^{14}N nuclei. Above room temperature, longitudinal relaxation times of the latter become long enough,

TABLE 1: Values of Selected Indirect Nuclear Spin–Spin Coupling Constants in 1

constant	absolute value (Hz)
$^1J(^{199}\text{Hg}-^{15}\text{N})^a$	316.2
$^2J(^{199}\text{Hg}-^{29}\text{Si})^b$	32.8
$^3J(^{199}\text{Hg}-^{13}\text{C})^c$	33.6
$^1J(^{29}\text{Si}-^{15}\text{N})^a$	9.4
$^1J(^{29}\text{Si}-^{13}\text{C})^c$	55.7
$^2J(^{15}\text{N}-^{14}\text{N})^d$	<9

^a Measured directly from the ^{199}Hg and ^{29}Si satellites, respectively, in the natural abundance ^{15}N NMR spectrum ($\pm 0.2 \text{ Hz}$), recorded by the refocused INEPT pulse sequence (based on $^3J(^{15}\text{N},\text{Si},\text{C},^1\text{H}) \approx 1.8 \text{ Hz}$) with ^1H decoupling. ^b Measured directly from the ^{199}Hg satellites in the ^{29}Si NMR spectrum ($\pm 0.2 \text{ Hz}$), recorded by the refocused INEPT pulse sequence (based on $^2J(^{29}\text{Si},\text{C},^1\text{H}) = 7 \text{ Hz}$), with ^1H decoupling. ^c Measured directly from the ^{199}Hg and ^{29}Si satellites, respectively, in $^{13}\text{C}\{^1\text{H}\}$ NMR spectrum ($\pm 0.2 \text{ Hz}$). ^d Determined from the spectrum at $T = 353 \text{ K}$ using the relationship $\Delta W = (8/3)J^2\pi T_{1Q}$ (see e.g. ref 15), where ΔW is the broadening of ^{15}N signal and T_{1Q} is the longitudinal relaxation time of the ^{14}N nucleus.

as compared with the magnitude of $^1J(^{199}\text{Hg}-^{14}\text{N}) = 226 \text{ Hz}$ calculated from the corresponding quantity in Table 1, for the line shapes of ^{199}Hg to become increasingly informative, along with further temperature increase, about the magnitudes of r at the individual temperatures. The computer routine to iterative line shape analysis, based on BWR theory, reported previously,⁸ is not applicable at hand to the present problem. This is because both ^{199}Hg and ^{14}N resonances in **1** are superpositions of contributions from a number of isotopomers in which these nuclei, beyond their mutual couplings, suffer additional scalar couplings to the ^{29}Si and ^{13}C nuclei. The relevant natural-abundance isotopomers of **1**, grouped into classes of the same spin coupling patterns to the ^{199}Hg and ^{14}N nuclei, are listed in Table 2. The above-mentioned computer routine was rendered capable of fitting a weighted sum of theoretical spectra, all of which are dependent on the same adjustable parameters, to the given experimental spectrum. Its capabilities were also extended to handle the spectra measured using the so-called Hahn echo technique (in which the pulse sequence preceding signal acquisition is also known as Carr–Purcell sequence A¹⁶). Our earlier experience, gained in solid-phase NMR line shape studies,¹⁷ is that some line shape details that are barely visible in standard spectra usually undergo amplification when one uses an experimental technique based on a delayed signal acquisition. In the present studies, due to accelerated quadrupolar relaxation, at temperatures below 333 K, the ^{199}Hg resonances gradually lose nontrivial features reflecting the degree of the quadrupolar cross-correlations while such features can still be discerned in the Hahn echo spectra measured for appropriately long echo times. However, this gain in the information content is at the cost of a substantial elongation of the experiment time, which is needed to achieve satisfactory signal-to-noise ratio.

Actually, we were able to determine r with relatively high accuracy in the range of 313° to 403 K , where the estimates of r at $T < 333 \text{ K}$ were obtained from Hahn echo spectra. Results of the line shape analyses are given in Table 3. Our present way of proceeding was as follows: At each temperature, we first performed line shape fits for the ^{14}N signal (the measurements of ^{199}Hg and ^{14}N spectra could be performed at exactly the same temperature because the same NMR probehead was used in each case). In these fits, the magnitudes of the relevant coupling constants were kept fixed; the only nontrivial parameter which was to be adjusted was the quadrupolar autocorrelation spectral density, j_a (in the extreme narrowing approximation which is applicable here, $20j_a = 1/T_{1Q} = 1/T_{2Q}$, see e.g., ref

TABLE 2: Natural-Abundance Isotomers of 1 Contributing to the Observed ^{199}Hg and ^{14}N Signals^a

^{199}Hg signal	statistical weight (%)	^{14}N signal	statistical weight (%)
$(\text{C}_3\text{Si})_2\text{NHg}^*\text{N}(\text{SiC}_3)_2$	72.16	$(\text{C}_3\text{Si})_2\text{NHgN}(\text{SiC}_3)_2$	68.07
$(\text{C}_3\text{Si})_2\text{NHg}^*\text{N}(\text{Si}^*\text{C}_3)(\text{SiC}_3)$	14.23	$(\text{C}_3\text{Si})_2\text{NHgN}(\text{Si}^*\text{C}_3)(\text{SiC}_3)$	13.43
$(\text{C}_3\text{Si})_2\text{NHg}^*\text{N}(\text{SiC}_2\text{C}^*)(\text{SiC}_3)$	9.70	$(\text{C}_3\text{Si})_2\text{NHg}^*\text{N}(\text{SiC}_3)_2$	12.82
$(\text{C}_3\text{Si})_2\text{NHg}^*\text{N}(\text{Si}^*\text{C}_2\text{C}^*)(\text{SiC}_3)$		$(\text{C}_3\text{Si})_2\text{NHg}^*\text{N}(\text{Si}^*\text{C}_3)(\text{SiC}_3)$	2.4
$(\text{C}_3\text{Si})_2\text{NHg}^*\text{N}(\text{SiC}_2\text{C}^*)(\text{Si}^*\text{C}_3)$	2.61		
$(\text{C}_3\text{Si})(\text{C}_3\text{Si}^*)\text{NHg}^*\text{N}(\text{SiC}_2\text{C}^*)(\text{SiC}_3)$			

^a Spin-1/2 isotopes of Hg, Si, and C are denoted by asterisks. The ^{201}Hg isotope is treated as magnetically nonactive because of its large quadrupole moment and, accordingly, extremely rapid quadrupolar relaxation in compounds with nonspherical electric field symmetry at the nuclear site. Contributions from isotomers whose relative abundances are below 1% are neglected.

TABLE 3: Auto- and Cross-Correlation Quadrupolar Spectral Densities Obtained from Lineshape Fits of NMR Spectra of ^{14}N and ^{199}Hg Nuclei in 1^a

T (K)	$j_a(\text{s}^{-1})$	$j_c(\text{s}^{-1})$	r
313	169.46 ± 0.31	126.9 ± 1.3	0.749 ± 0.007
323	146.27 ± 0.25	111.8 ± 0.6	0.764 ± 0.004
333	128.55 ± 0.31	94.2 ± 0.6	0.733 ± 0.005
343	108.32 ± 0.25	84.2 ± 0.6	0.777 ± 0.006
363	85.07 ± 0.19	66.6 ± 0.6	0.783 ± 0.008
383	67.92 ± 0.19	54.0 ± 0.6	0.795 ± 0.010
403	54.73 ± 0.19	42.1 ± 0.6	0.769 ± 0.011

^a Errors listed in columns 2 and 3 are standard errors delivered by the fitting routine; they may be underestimated because of possible statistical cross-correlations between the estimates of j_a and j_c , and those of the remaining line shape parameters.

18). From the theoretical considerations confirmed by numerical simulations,⁷ it is known that in systems such as that considered presently the signal of the quadrupolar nuclei is independent of the quadrupolar cross-correlation spectral density, j_c (where $j_c/j_a = r$). The value of j_a was then used as a nonadjustable parameter in the line shape fit of the ^{199}Hg signal. Here the only nontrivial adjustable parameter was j_c . As was once deduced from the theoretical considerations cited above,⁷ which were recently confirmed by experimental findings,⁸ the estimate of j_c delivered at convergence may be critically dependent on the absolute value of the J-coupling constant between the quadrupolar nuclei, especially in the instance where the latter are magnetically equivalent. In the present studies, we could only assess the absolute value of $J(^{14}\text{N}-^{14}\text{N})$ to be smaller than 6 Hz (see Table 1). Our estimates of j_c obtained assuming various values of $J(^{14}\text{N}-^{14}\text{N})$ from the range 0–6 Hz did not differ among themselves by more than 0.5%. However, assuming an unrealistic value of $J(^{14}\text{N}-^{14}\text{N})$ to be greater than 30 Hz leads to an increase of the estimated value of j_c by more than 7%. One more point that needs to be commented upon in the present context involves the impact on the estimated values of j_a and j_c of the line broadenings caused by factors other than quadrupolar relaxation. While the field inhomogeneity broadenings, the magnitudes of which we can assess to be smaller than 0.5 Hz, are of little significance, those originating from relatively fast ^{199}Hg relaxation, dominated by the CSA mechanism, are nonnegligible, especially at low temperatures. To make a proper account of these CSA-relaxation broadenings in our line shape fits, we performed independent measurements of the longitudinal relaxation times of ^{199}Hg , which are described in the next subsection. In the line shape fits, the CSA-relaxation effects on the ^{199}Hg resonances were accounted for as Lorentzian broadenings $w(\text{Hz}) = 7/(6\pi T_1)$.¹⁵

For selected temperatures, the experimental ^{199}Hg and ^{14}N spectra with the superimposed “best fit” theoretical spectra are displayed in Figure 2. It must be added that these solutions of the least-squares problems for the ^{199}Hg spectra are not unique. When negative values of j_c are assumed at the start, the

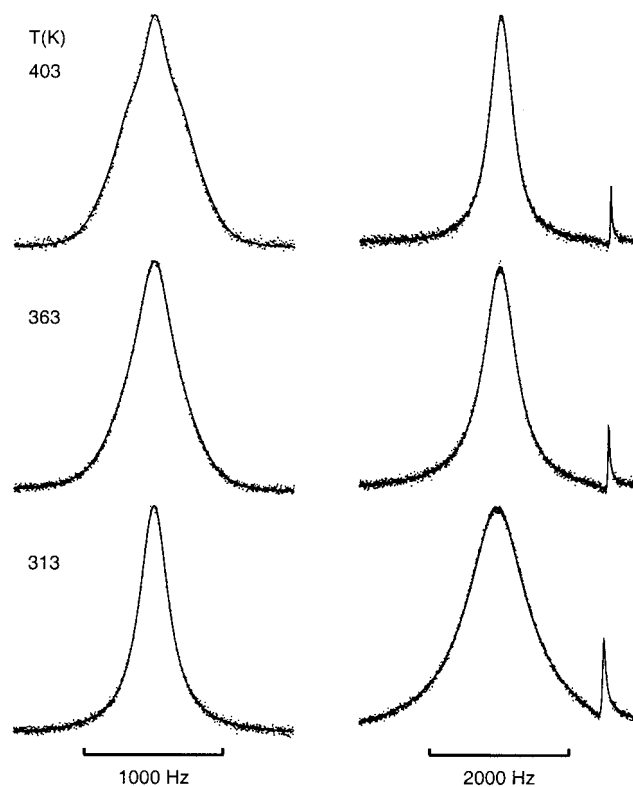


Figure 2. Experimental ^{199}Hg (left side) and ^{14}N (right side) spectra of toluene solution of **1** for selected temperatures, and the superimposed “best fit” theoretical spectra. The ^{199}Hg spectra at $T = 313$ K are the Hahn echo spectra (see text). Lorentzian line shape was assumed for the narrow impurity signal (originating from admixture of the free ligand) in the ^{14}N spectra.

corresponding values delivered at convergence are also negative, and their absolute magnitudes are nearly the same as those obtained from positive starting values. These “negative” solutions have been rejected since the corresponding rms errors were consistently larger, by 1 to 7%, than those achieved for the respective “positive” solutions.

Longitudinal Relaxation Times. T_1 relaxation times of ^{199}Hg in **1** were measured in temperature range of 243 to 403 K using the standard inversion recovery technique. In **1** as in other covalent compounds of ^{199}Hg ,¹⁹ the relaxation behavior of this nucleus is dominated by the CSA mechanism. An Arrhenius plot of the observed ^{199}Hg relaxation rates is shown in Figure 3. The deviations of the experimental relaxation rates from the least-squares straight line (described in caption to Figure 3) do not seem to bear a systematic character. They can be attributed to random errors in determining the integral intensities of the relatively broad ^{199}Hg resonances for the recovery times at which the magnetization recovery curves cross zero.

At temperatures below the room temperature, the relaxation times of the ^{14}N nuclei become too short to be measured with

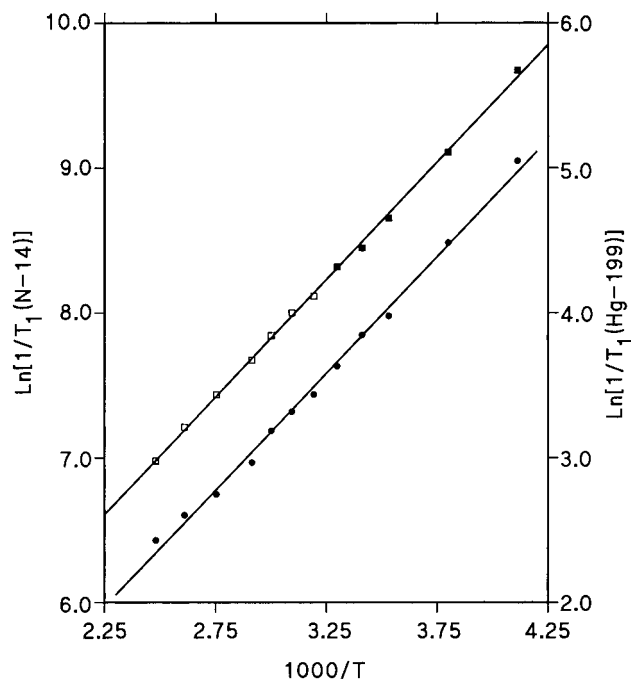


Figure 3. Arrhenius plots of the ^{199}Hg (solid circles) and ^{14}N (squares) relaxation rates $1/T_1$ (s^{-1}). The corresponding least-squares regression lines are: $\ln(T_1) = -(13.41 \pm 0.25 \text{ kJ mol}^{-1})/RT + (1.66 \pm 0.11)$ and $\ln(T_1) = -(13.49 \pm 0.13 \text{ kJ mol}^{-1})/RT - (2.96 \pm 0.06)$. Open and solid squares designate data obtained from line shape fits of ^{14}N and ^{199}Hg spectra, respectively (see text).

reasonable accuracy using either the inversion recovery or the line shape analysis technique. In this temperature range, the longitudinal relaxation times (and, in fact, the j_a parameters) were determined indirectly from line shape fits of the ^{199}Hg signals. In these fits, the parameter j_a was varied while the values j_c were set equal to $r_{\text{av}}j_a$, where r_{av} is an arithmetic average of the estimates of r obtained at temperatures above the room temperature. As in the line shape fits carried out to determine r , the broadening of the ^{199}Hg spectra due to the CSA relaxation was calculated from the independently measured longitudinal relaxation times of the ^{199}Hg nucleus. The bias of the estimated values of j_a caused by fixing the magnitude of r is negligible since in the temperature range considered line shapes of the ^{199}Hg spectra measured in the standard way are essentially insensitive to r . An Arrhenius plot of the longitudinal relaxation rates of the ^{14}N nuclei is shown in Figure 3. As can be seen in Figure 3, the experimental points are nearly perfectly aligned along a straight line. It is noteworthy that the slope of the latter is practically identical with that of corresponding line for the ^{199}Hg relaxation rates (see caption to Figure 3).

The ^{29}Si and ^{13}C Spectra. In both ^{29}Si and ^{13}C spectra, the satellite lines due to coupling with the ^{199}Hg nucleus do not show any extra broadening beyond that caused by relatively rapid longitudinal relaxation of ^{199}Hg . This holds true even for the highest temperature, $T = 403 \text{ K}$, at which such spectra were measured. These observations allow us to exclude the occurrence of intermolecular ligand exchange; in the cadmium analogue of **1**, such process does occur in toluene solutions of comparable molecular concentration, causing significant broadenings and, at elevated temperatures, collapses of the corresponding ^{13}C and ^{29}Si doublets into singlets.

Discussion

For a molecule whose structure is rigid on the time scale of molecular tumbling, cross-correlations between various time-

dependent intramolecular interactions that contribute to nuclear spin relaxation are in general dependent on both geometrical and dynamic factors. These include orientations of the corresponding interaction tensors relative to the principal axis system of the rotational diffusion (RD) tensor, and the anisotropy of the latter. In the specific instance where such a molecule possesses symmetry center, the pairs of interactions whose respective tensors are transformed into each other under inversion in the center remain perfectly cross-correlated; as was once shown theoretically,²⁰ this holds true for any microscopic mechanism of rotational diffusion and any symmetry of the RD tensor. Such perfect cross-correlations would be maintained even in the presence of intramolecular motions provided that the latter are sufficiently fast as compared with the overall tumbling. In typical situations, upon changing the temperature the rates of the overall reorientation would be affected more substantially than those of the fast intramolecular processes. By an increase of temperature, the original disparity between the corresponding time scales might be diminished, which could manifest itself in a gradual decorrelation of the symmetry-related interactions.

For the compound investigated presently, we were able to evaluate the quadrupolar cross-correlation coefficient, r , in the temperature range over which the overall tumbling, monitored by the ^{199}Hg relaxation rate (see below) is accelerated by more than a factor of 3. However, the estimated values of r , all of which fall below 0.8, do not show any systematic increase toward the limiting value 1 along with decreasing the temperature from 403 down to 313 K. Actually, to within the corresponding triple standard errors they remain independent of temperature. These observations can be rationalized if one assumes that the $\text{Si}_2\text{NHgNSi}_2$ skeleton behaves like a rigid body on the time scale of the molecular reorientations that are relevant for quadrupolar relaxation. In agreement with the inferences from the ED data for gas phase,^{11–13} the possibility that it exists in D_{2h} conformation ought to be excluded because the values of r are substantially different from 1. Moreover, regardless of what is the true conformation of **1**, the possibility that the EFG tensors for the ^{14}N nuclei are axially symmetric around the N–Hg–N axis should also be excluded since otherwise the values of r would be close to unity. However, the above conclusions are rather critically dependent on how realistic is the assumption about an essential rigidity of the $\text{Si}_2\text{NHgNSi}_2$ skeleton. To verify it further, we measured longitudinal relaxation times for the ^{14}N and ^{199}Hg nuclei, which could be done over much broader temperature range, i.e., 243 to 403 K, than for r .

Over the whole range, a perfect parallelism between the dependences on temperature of the ^{14}N and ^{199}Hg relaxation rates is maintained (see Figure 2). As is pointed out below, this observation provides another essential argument against a flexibility of the $\text{Si}_2\text{NHgNSi}_2$ fragment (anticipated in view of the occurrence of large-amplitude librations in gas phase^{11–13}) on a time scale commensurable with that of molecular tumbling. Let us note that, because the N–Hg bond is essentially a single bond,^{10,14} the CSA tensor of the ^{199}Hg nucleus can to a good approximation be regarded as axially symmetric around the N–Hg–N axis, regardless of what is the true conformation of **1** (for D_{2d} conformation, this would be an exact symmetry). For any mutual orientation of the HgNSi_2 groups, the latter, which will further be referred to as Z axis, will remain an effective symmetry axis of the whole molecule. Hence, the relaxation behavior of the ^{199}Hg nucleus will be controlled by reorientations around axes perpendicular to Z axis and will be insensitive to any motions around it. On the other hand,

reorientations around Z must contribute to the relaxation rates of the ^{14}N nuclei, since the possibility for the EFG tensors to be axially symmetric with respect to the latter must be rejected (see above). Therefore, the parallelism between the ^{199}Hg and ^{14}N relaxation behaviors could be rationalized when reorientations around Z and around the axes perpendicular to it were controlled by the same microscopic mechanism. Our experimental findings seem to confirm the occurrence of such a single mechanism. Its temperature behavior follows Arrhenius law rather closely, what can be seen from the Arrhenius plots of the ^{14}N and ^{199}Hg relaxation rates shown in Figure 3, revealing the same activation energy of 13.4 kJ mol^{-1} . This points to an essential irrelevance for the observed relaxation effects of the possible large-amplitude librations around Z . In liquid phase, such librations can be considered in terms of some large-angle, rotational jumps modulating the small-angle, diffusional reorientations around Z . Such jumps would affect the ^{14}N relaxation rates only, via the asymmetries of the corresponding EFG tensors; because of axial symmetry around Z of the CSA tensor, they would not be reflected in relaxation rates of the ^{199}Hg nucleus. It is highly unlikely that the temperature dependence of such jumps be exactly the same as for diffusional reorientations. Thus, the temperature behavior of the ^{14}N and ^{199}Hg relaxation rates discussed above, observed over temperature range exceeding 150 K , can be rationalized if the mean lifetime of the molecules of **1** between the possible large-angle jumps happens to be much longer than the orientational correlation time for the small-angle diffusion. This may mean that the relatively low, ca. 8 kJ mol^{-1} , librational barrier found in gas phase¹¹ is substantially increased in liquid phase due to intermolecular interactions. In conclusion, in the observed relaxation behavior of the system discussed there are no such features that would necessitate going beyond the standard interpretation in terms of rotational diffusion. Moreover, the data collected reveal no flexibility of the $\text{Si}_2\text{NHgNSi}_2$ fragment on the time scale of the overall molecular tumbling. In view of what was pointed out at the beginning of this section, and of the fact that structures with the two NSi_2 groups permanently twisted relative to each other by angles different from 90° are highly improbable, one is left with the D_{2d} geometry as the only possibility for the conformation of the $\text{Si}_2\text{NHgNSi}_2$ skeleton. This is in agreement with the inferences from the gas-phase studies.^{11–13}

Detailed questions regarding the nature of the rotational diffusion mechanism of the molecules of **1** and, more specifically, whether it is dominated by purely inertial^{21,22} or microviscosity effects,^{23,24} must be left open. Nevertheless, in accord with D_{2d} geometry, axial symmetry around Z axis is to be assumed for the relevant RD tensor; in what follows, the two diffusion constants characterizing reorientations around Z , and around axes perpendicular to Z , will be denoted by D_{\parallel} and D_{\perp} , respectively. Now, for each of the ^{14}N nuclei, one of the principal axes of its EFG tensor will be directed along Z while the two remaining axes, perpendicular to Z , will lie in the symmetry planes of the corresponding NSi_2 groups (see inset in Figure 1). The system of the two principal axes perpendicular to Z of each EFG tensor is twisted by the angle of 90° relative to the corresponding system of the other. Using the expressions for auto- and cross-correlation spectral densities that are applicable to interaction tensors without axial symmetry,^{25,26} one can derive relationships connecting the observed values of r with both the RD anisotropy parameter $\xi = D_{\parallel}/D_{\perp}$ and the characteristics of the EFG tensors. For any such tensor, it is customary to label its principal axes in such a way that the

absolute magnitudes of the corresponding principal values be ordered according to:¹⁵

$$|V_{xx}| \leq |V_{yy}| \leq |V_{zz}| \quad (1)$$

Then, the corresponding EFG asymmetry parameter $\eta = (V_{xx} - V_{yy})/V_{zz}$ is nonnegative and never exceeds 1. Depending on which of the three principal EFG axes, x , y , and z , whose associated principal values obey eq 1, happens to coincide with the Z axis of the RD tensor, a different functional dependence of r on η and ξ is obtained. All these three relationships can be described by a single expression

$$r = \frac{1 - \lambda_u(\eta)/(1 + 2\xi)}{1 + \lambda_u(\eta)/(1 + 2\xi)} \quad (2)$$

where for the orientations of $x||Z$, $y||Z$, and $z||Z$, the corresponding functions λ_x , λ_y , and λ_z , are $[(3 + \eta)/(1 - \eta)]^2$, $[(3 - \eta)/(1 + \eta)]^2$ and η^2 , respectively. Our experimental results, combined with an assessment of the probable magnitudes of the motional anisotropy parameter ξ , allow one to discriminate between these three orientations. Namely, if the gradient of the smallest magnitude was along Z axis (i.e., $x||Z$), then only for the values of ξ exceeding 40 eq 2 would deliver physically sensible values of η (i.e., ones fulfilling $0 \leq \eta \leq 1$). It is worth noting that the smallest value of ξ , that is, ca. 40, would correspond to the limiting situation where each of the EFG tensors was axially symmetric ($\eta = 0$) around an axis perpendicular to Z (with the axes of the individual tensors subtending a dihedral angle of 90° , see above); for the values of η approaching 1 the corresponding values of ξ would tend to infinity. As is pointed out below, such an extent of rotational asymmetry for the molecules of **1** is extremely unlikely, so that the possibility of x being parallel to Z can be excluded. For the hypothetical orientation of $y||Z$, the limiting values of ξ are about 4 (for $\eta = 1$) and about 40 (for $\eta = 0$, in which instance the orientations $y||Z$ and $x||Z$ become nondifferentiable by definition). It is illuminating to compare these estimates of ξ with the predictions derived from the two already invoked theoretical models of anisotropic rotational diffusion in liquids, the extended rotational diffusion (ERD) in the limit of small angle displacements,²² and hydrodynamic (HD)^{23,24} models. In the former, the anisotropy parameter ξ is given by the ratio of the corresponding principal values of the molecular inertia tensor $I_x/I_z (= I_y/I_z)$; for the gas-phase geometry of **1**, the value of ξ calculated in this way amounts to ca. 2.5. In various versions of the HD model, the motional anisotropy is related to the anisotropy of the molecular shape; for molecules of approximately spherical shape isotropic reorientation is predicted, regardless of the properties of the molecular inertia tensor. In the D_{2d} conformation, the molecules of **1** are approximately spherical. Moreover, they do not contain any peripheral functional groups that might engage in specific interactions with the solvent molecules, which would render the HD approach inapplicable. In any case, it seems reasonable to assume that the value of ξ falls somewhere between 1 (isotropic reorientation) and 2.5. Therefore, the possibility of $y||Z$ can also be excluded and, accordingly, the most likely orientation of the EFG tensor for each of the ^{14}N nuclei is such that the axis of maximum gradient is directed along the N–Hg bond ($z||Z$). Putting for r in eq 2 the arithmetic average of the corresponding values from Table 3, 0.77, the values of η falling in the range of 0.62 (for isotropic reorientation, $\xi = 1$) to 0.88 (for $\xi = 2.5$) are obtained. Thus, even such a nonprecise assessment of the reorientational asymmetry can yield reasonable estimates of η .

To the best of our knowledge, this is the first attempt of determining the properties of an EFG tensor from quadrupolar cross-correlation effects in an isotropic liquid.

Conclusions

The data on temperature dependences of both the quadrupolar cross-correlation and longitudinal relaxation of ^{14}N and ^{199}Hg nuclei for a toluene solution of **1** are shown to be consistent with the structure in which the $\text{Si}_2\text{N}-\text{Hg}-\text{NSi}_2$ skeleton maintains D_{2d} geometry on the time scale of overall molecular reorientation. The extent of the possible anisotropy of the latter, described by the ratio $\xi = D_{\parallel}/D_{\perp}$ of the relevant rotational diffusion constants, must be confined to relatively narrow limits: from isotropic reorientation ($\xi = 1$) expected from hydrodynamic models to the anisotropy controlled by the properties of the moment of inertia tensor, in which case ξ ought not to exceed 2.5. Accordingly, the principal axes of the ^{14}N EFG tensors, concerned with gradients of maximum absolute values, can uniquely be located along the direction of the $\text{N}-\text{Hg}-\text{N}$ chain. The value of the EFG asymmetry parameter, calculated from the experimental data assuming isotropic reorientation, amounts to 0.62. The present work seems to provide the first evidence of the utility of quadrupolar cross-correlation effects for structural studies in isotropic liquids.

Acknowledgment. This work was sponsored in part by the State Committee for Scientific Research (KBN) under Grant No. 3T09A 096 15.

References and Notes

- (1) Kumar, A.; Christy Rani Grace, R.; Madhu, P. K. *Prog. NMR Spectrosc.* **2000**, *37*, 191.
- (2) Poupko, R.; Vold, R. L.; Vold, R. R. *J. Magn. Reson.* **1979**, *34*, 67.
- (3) Vold, R. L.; Vold, R. R.; Poupko, R.; Bodenhausen, G. *J. Magn. Reson.* **1980**, *38*, 14.

- (4) ter Beek, R. C.; Burnell, E. E. *Phys. Rev. B* **1994**, *50*, 9245.
- (5) Wangsness, R. K.; Bloch, F. *Phys. Rev.* **1953**, *89*, 728. Bloch, F. *Phys. Rev.* **1956**, *102*, 204; *Phys. Rev.* **1957**, *105*, 1206.
- (6) Redfield, A. G. *Adv. Magn. Reson.* **1965**, *1*, 1.
- (7) Szymański, S. *J. Magn. Reson.* **1997**, *127*, 199.
- (8) Bernatowicz, P.; Bjorlo, O.; Morkved, E. H.; Szymański, S. *J. Magn. Reson.* **2000**, *145*, 152.
- (9) Bernatowicz, P.; Szymański, S. *J. Magn. Reson.* **2001**, *148*, 455.
- (10) Burger, H.; Sawodny, W.; Wannagat, U. *J. Organomet. Chem.* **1965**, *3*, 113.
- (11) Aleya, E. C.; Fisher, K. J.; Fjeldberg, T. *J. Mol. Struct.* **1985**, *130*, 263.
- (12) Aleya, E. C.; Fisher, K. J.; Fjeldberg, T. *J. Mol. Struct.* **1985**, *127*, 325.
- (13) Haaland, A.; Hedberg, K.; Power, P. P. *Inorg. Chem.* **1984**, *23*, 1972.
- (14) Harris, D. H.; Lappert, M. F.; Pedley, J. B.; Sharp, G. J. *J. Chem. Soc., Dalton Trans.* **1976**, 945.
- (15) Abragam, A. *The Principles of Nuclear Magnetism*; Clarendon Press: Oxford, 1962.
- (16) See e.g. Ernst, R. R.; Bodenhausen, G.; Wokaun, A. *Principles of nuclear magnetic resonance in one and two dimensions*; Clarendon Press: Oxford, 1987; p. 208; the acquisition of the NMR signal is delayed by time interval 2τ from stimulating $\pi/2$ radio frequency pulse which is followed by a π pulse applied at time τ (obviously, in calculating the line shape, the evolution of the spin system during this 2τ interval, including effects of the π pulse, is taken into account).
- (17) Szymański, S.; Olejniczak, Z.; Detken, A.; Haeberlen, U. *J. Magn. Reson.* **2001**, *148*, 277.
- (18) Werbelow, L. G. in *Encyclopedia on Nuclear Magnetic Resonance*; Grant, D. M., Harris, R. K., Eds.; Wiley: Chichester, 1996; p 4092.
- (19) Benn, R.; Guenther, H.; Maercker, A.; Menger, V.; Schmitt, P. *Angew. Chem.* **1982**, *94*, 314; *Angew. Chem., Int. Ed. Engl.* **1982**, *21*, 295.
- (20) Szymański, S.; Gryff-Keller, A. M.; Binsch, G. *J. Magn. Reson.* **1986**, *68*, 399.
- (21) Gordon, R. G. *J. Chem. Phys.* **1966**, *44*, 1830.
- (22) McClung, R. E. D. *Adv. Mol. Relaxation Interaction Processes* **1977**, *10*, 83.
- (23) Youngren, G. K.; Acrivos, A. *J. Chem. Phys.* **1975**, *63*, 3846.
- (24) Kluner, R. P.; Dolle, A. *J. Phys. Chem. A* **1997**, *101*, 1657.
- (25) Werbelow, L. G. in *Nuclear Magnetic Resonance Probes of Molecular Dynamics*; Tycko, R., Ed.; Kluwer Academic: Dordrecht, 1994; Chapter 5.
- (26) Canet, D. *Concepts Magn. Reson.* **1998**, *10*, 291.